

Loss of $G_s\alpha$ in the Postnatal Skeleton Leads to Low Bone Mass and a Blunted Response to Anabolic Parathyroid Hormone Therapy*

Received for publication, July 17, 2015, and in revised form, November 19, 2015. Published, JBC Papers in Press, November 23, 2015, DOI 10.1074/jbc.M115.679753

Partha Sinha[‡], Piia Aarnisalo^{‡§}, Rhiannon Chubb[‡], Ingrid J. Poulton[¶], Jun Guo[‡], Gregory Nachtrab[‡], Takaharu Kimura^{||}, Srilatha Swami^{||}, Hamid Saeed^{||}, Min Chen^{**}, Lee S. Weinstein^{**}, Ernestina Schipani^{††}, Natalie A. Sims[¶], Henry M. Kronenberg[‡], and Joy Y. Wu^{‡||1}

From the [‡]Endocrine Unit, Massachusetts General Hospital, Boston, Massachusetts 02114, [§]Department of Clinical Chemistry, University of Helsinki and Helsinki University Central Hospital, Hospital District of Helsinki and Uusimaa, Laboratory Services, HUSLAB, 00029 HUS, Finland, [¶]St. Vincent's Institute and Department of Medicine at St. Vincent's Hospital, The University of Melbourne, Fitzroy, Victoria, Australia, ^{||}Division of Endocrinology, Stanford University School of Medicine, Stanford, California 94305, ^{**}Metabolic Diseases Branch, NIDDK, National Institutes of Health, Bethesda, Maryland 20892, and ^{††}Departments of Orthopedic Surgery and Medicine, University of Michigan, Ann Arbor, Michigan 48109

Parathyroid hormone (PTH) is an important regulator of osteoblast function and is the only anabolic therapy currently approved for treatment of osteoporosis. The PTH receptor (PTH1R) is a G protein-coupled receptor that signals via multiple G proteins including $G_s\alpha$. Mice expressing a constitutively active mutant PTH1R exhibited a dramatic increase in trabecular bone that was dependent upon expression of $G_s\alpha$ in the osteoblast lineage. Postnatal removal of $G_s\alpha$ in the osteoblast lineage (P- $G_s\alpha^{\text{OsxKO}}$ mice) yielded markedly reduced trabecular and cortical bone mass. Treatment with anabolic PTH(1–34) (80 $\mu\text{g}/\text{kg}/\text{day}$) for 4 weeks failed to increase trabecular bone volume or cortical thickness in male and female P- $G_s\alpha^{\text{OsxKO}}$ mice. Surprisingly, in both male and female mice, PTH administration significantly increased osteoblast numbers and bone formation rate in both control and P- $G_s\alpha^{\text{OsxKO}}$ mice. In mice that express a mutated PTH1R that activates adenylyl cyclase and protein kinase A (PKA) via $G_s\alpha$ but not phospholipase C via $G_{q/11}$ (D/D mice), PTH significantly enhanced bone formation, indicating that phospholipase C activation is not required for increased bone turnover in response to PTH. Therefore, although the anabolic effect of intermittent PTH treatment on trabecular bone volume is blunted by deletion of $G_s\alpha$ in osteoblasts, PTH can stimulate osteoblast differentiation and bone formation. Together these findings suggest that alternative signaling pathways beyond $G_s\alpha$ and $G_{q/11}$ act downstream of PTH on osteoblast differentiation.

Osteoporosis is one of the most common degenerative diseases of aging with an estimated 50% of postmenopausal

women and 25% of older men at risk of sustaining a fragility fracture and economic costs exceeding \$19 billion annually in the United States (1). The low bone mass underlying osteoporosis results from an imbalance between bone formation and bone resorption that leads to bone loss that becomes more pronounced with age (2). The most commonly prescribed therapies for osteoporosis target the inhibition of bone resorption but as such are not curative.

Anabolic therapy to increase osteoblast numbers and function and thereby stimulate bone formation is appealing as a potential route to curing osteoporosis. Administered once daily, recombinant parathyroid hormone (PTH(1–34);² teriparatide) reduces fracture risk and significantly increases bone mineral density and bone mass (3). Teriparatide is currently the only Food and Drug Administration-approved anabolic therapy for osteoporosis. However, the mechanisms by which intermittent PTH stimulates bone anabolism have not been fully clarified.

Intermittent PTH treatment enhances bone formation and increases osteoblast numbers by a variety of mechanisms including stimulation of osteoblast proliferation and differentiation, inhibition of osteoblast apoptosis, and activation of quiescent lining cells (4–11). PTH also suppresses the expression of sclerostin, an inhibitor of canonical Wnt signaling produced by osteocytes and encoded by the *Sost* gene (12, 13). Canonical Wnt signaling plays a crucial role in regulating osteoblast differentiation and bone formation (14–16), and patients lacking sclerostin have high bone mass (17, 18). Highlighting the clinical relevance of this pathway, neutralizing antibodies targeted against sclerostin are now in clinical trials for the treatment of osteoporosis (17–19) and are being tested in preclinical models

* This work was supported by National Institutes of Health Grants AR054741 and AR059942 (to J. Y. W.), AR061228 (to P. S.), and DK011794 (to H. M. K.) and the NIDDK Intramural Research Program (to M. C. and L. S. W.). The authors declare that they have no conflicts of interest with the contents of this article. The content is solely the responsibility of the authors and does not necessarily represent the official views of the National Institutes of Health.

¹ To whom correspondence should be addressed: Division of Endocrinology, Stanford University School of Medicine, 300 Pasteur Dr., S-025, Stanford, CA 94305. Tel.: 650-736-9654; Fax: 650-725-7085; E-mail: jywu1@stanford.edu.

² The abbreviations used are: PTH, parathyroid hormone; PTH1R, PTH receptor; PLC, phospholipase C; caPTH1R, constitutively active mutant form of PTH1R; Osx, osterix; μCT , micro-computed tomography; BV, bone volume; TV, tissue volume, BV/TV, trabecular bone volume fraction; Tb.Th, trabecular thickness; Tb.Sp, trabecular separation; Tb.N, trabecular number; Co.Th, cortical thickness; P1NP, procollagen type I N-terminal propeptide; CTX, type I collagen C-terminal telopeptide; SOST, sclerostin; *Colla1*, collagen $\alpha 1$; *Opn*, osteopontin; *Bglap*, osteocalcin.

Low Bone Mass in Mice Lacking $G_s\alpha$ in the Postnatal Skeleton

of other conditions of bone fragility such as osteogenesis imperfecta (20, 21).

The PTH receptor PTH1R is a G protein-coupled receptor. Stimulation of PTH1R by PTH activates a variety of G proteins including the stimulatory G protein G_s . G_s activates adenylyl cyclase, thereby increasing cyclic AMP (cAMP) levels and activating the protein kinase A (PKA) gene transcription pathway (22). Several lines of evidence suggest that G_s is a major mediator of the anabolic actions of PTH. PTH induces the expression of several osteoblast-specific target genes including osteocalcin (*Bglap*) (23), *Mmp13* (24), and *Tnfsf11* (25) in a PKA-dependent manner. Targeting of a constitutively active mutant form of PTH1R (caPTH1R), identified in patients with Jansen metaphyseal chondrodysplasia, to osteoblasts in mice results in profound increases in trabecular bone mass (26). *In vitro*, this mutant version of PTH1R predominantly activates G_s -dependent signaling pathways (27). Furthermore, constitutive activation of G_s -dependent signaling by an engineered G_s -coupled receptor also significantly increases trabecular bone mass (28). In addition to G_s , PTH1R couples to several other G proteins, activating phospholipase $C\beta$ via G_q/G_{11} to stimulate protein kinase C and G_{12}/G_{13} to stimulate phospholipase D (29, 30). We have previously reported that phospholipase C (PLC) signaling via PTH1R is essential for stromal cell response to PTH in growing mice (31). Activation of PTH1R also recruits β -arrestins 1 and 2, leading to receptor internalization and activation of ERK1/2 (32).

In the osteoblast lineage, the α subunit of the heterotrimeric G_s protein $G_s\alpha$ is required for normal skeletal development during embryogenesis (33–35). Deletion of $G_s\alpha$ early in the osteoblast lineage using Cre recombinase under control of the osterix (*Osx*) promoter (16) markedly impairs bone formation such that more immature woven bone is observed (35). There are at least two distinct roles for $G_s\alpha$ in the osteoblast lineage during skeletal development. $G_s\alpha$ is required for commitment of mesenchymal progenitors to the osteoblast lineage rather than the adipocyte lineage, likely mediated at least in part by alterations in Wnt signaling (33, 35). In contrast, in cells committed to the osteoblast lineage, $G_s\alpha$ restrains osteoblast differentiation (35).

Constitutive activation of G_s -dependent signaling in osteoblasts throughout embryogenesis results in a dramatic increase in trabecular bone volume (28). However, when activation of G_s is delayed until birth, there is a much milder increase in bone (36), and if delayed until 4 weeks of age, there is no discernible skeletal phenotype (28). Therefore $G_s\alpha$ -dependent signaling may have different functions during embryogenesis compared with postnatal skeletal homeostasis. Mice with $G_s\alpha$ deleted throughout embryonic development in *Osx*-expressing osteoprogenitors die before weaning (35). By administering doxycycline to suppress the expression of Cre recombinase, we delayed ablation of $G_s\alpha$ in the osteoblast lineage until birth (postnatal or P- $G_s\alpha^{\text{OxskKO}}$ mice), allowing us to examine the role of $G_s\alpha$ in osteoblasts in the postnatal skeleton. Here we report that $G_s\alpha$ is required for the high trabecular bone mass observed with constitutive activation of PTH1R. P- $G_s\alpha^{\text{OxskKO}}$ mice have severe osteoporosis, and when treated with anabolic PTH, there was no increase in trabecular bone volume or cortical thickness.

However, osteoblast numbers and bone formation rate still increased along the trabecular surface of P- $G_s\alpha^{\text{OxskKO}}$ mice. We also examined the effects of anabolic PTH on PLC-defective mutant (D/D) mice that express only a mutated PTH1R that activates adenylyl cyclase normally but cannot activate PLC and found that PTH significantly increased almost all parameters of bone formation in tibiae of both wild type (WT) and D/D mice. Together these data demonstrate the involvement of other downstream mediators beyond activation of PKA and protein kinase C (PKC) in the anabolic action of PTH.

Experimental Procedures

Mice—Generation of $G_s\alpha^{\text{OxskKO}}$ mice has been described previously (34, 35). Postnatal deletion of $G_s\alpha$ was achieved by administering 10 $\mu\text{g}/\text{ml}$ doxycycline in drinking water from conception until birth. Rosa26 (R26R, stock 3309) (37) and mTmG reporter mice (38) were obtained from The Jackson Laboratory (Bar Harbor, ME). Because $G_s\alpha^{\text{OxskKO}}$ mice are of mixed genetic background, littermate controls ($G_s\alpha(\text{fl/fl})$) except where otherwise specified) were used for all experiments described. Generation of D/D mice has been described previously (39). Genotyping was performed on tail genomic DNA using protocols published previously (34, 35, 39). All animals were housed in the Center for Comparative Medicine at the Massachusetts General Hospital where all experiments were approved by the hospital's Subcommittee on Research Animal Care or at the Veterinary Services Center at Stanford University School of Medicine where all experiments were approved by the Stanford Administrative Panel on Laboratory Animal Care.

Histology—Mouse limbs were fixed in 10% buffered formalin, paraffin-embedded, and sectioned. Immunohistochemical analysis was performed on deparaffinized sections using biotinylated mouse anti-SOST antibody (R&D Systems). For X-Gal staining of β -galactosidase activity, limbs were fixed in 0.2% glutaraldehyde and 1.5% formaldehyde followed by overnight staining at 37 °C in X-Gal solution containing 1 mg/ml X-Gal (Takeda, Osaka, Japan), 5 mM potassium ferricyanide, 5 mM potassium ferrocyanide, 2 mM MgCl_2 , 0.01% sodium deoxycholate, and 0.02% Nonidet P-40 (10).

Skeletal Preparations—Skeletons were fixed in 95% ethanol and then stained overnight in 0.015% Alcian blue in acetic acid/ethanol to highlight cartilage. Soft tissues were cleared in 1% KOH and then stained overnight in 0.01% alizarin red to detect mineralized bone (40).

Bone Mineral Density—Mice were anesthetized with tribromoethanol (600 mg/kg). Bone mineral density of the whole skeleton (excluding calvariae) or individual bones was measured by dual energy x-ray absorptiometry on a Lunar Piximus (GE Medical Systems, Milwaukee, WI).

Micro-computed Tomography (μCT) Analysis—Assessment of bone morphology and microarchitecture was performed using a desktop high resolution μCT ($\mu\text{CT}40$, Scanco Medical, Brüttisellen, Switzerland) as described previously (41). Briefly, the distal femoral metaphysis (P- $G_s\alpha^{\text{OxskKO}}$ mice) or L5 vertebrae (D/D mice) was scanned for trabecular bone assessment, and mid-diaphyses were scanned for cortical bone assessment using x-ray energy of 70 KeV, an integration time of 200 ms, and a 12- μm isotropic voxel size. Trabecular bone volume fraction

(BV/TV), trabecular thickness (Tb.Th), trabecular separation (Tb.Sp), and trabecular number (Tb.N) were calculated using a threshold computed for control samples. For cortical bone analysis, cortical thickness (Co.Th) was assessed using a pre-defined fixed threshold.

Histomorphometry—Double calcein labeling was performed by injecting mice with 20 mg/kg calcein 3 and 10 days before sacrifice. Bones were fixed in 10% buffered formalin and embedded in methylmethacrylate as described previously (42). 5- μ m sections were stained with toluidine blue or xylenol orange. Histomorphometric analysis of undecalcified trabecular bone was performed using the Osteomeasure system (OsteoMetrics, Decatur, GA) (42).

Quantitative Real Time PCR—Total RNA was prepared from flushed long bones and primary osteoblasts using the RNeasy kit (Qiagen), and cDNA was synthesized with the SuperScript III First Strand synthesis system for real time PCR (Invitrogen). Quantitative real time PCR was performed using primers for *Gnas* (43), *Runx2* (44), *Osx* (44), collagen I α 1 (*Coll1 α 1*) (40), osteopontin (*Opn*) (44), osteocalcin (*Bglap*) (45), and *Sost* (46) according to previously published protocols with mRNA levels normalized relative to β -actin expression. Total RNA samples subjected to cDNA synthesis reactions in the absence of reverse transcriptase were included as negative controls.

Serum Biochemistries—Blood was harvested by cardiac puncture at the time of euthanasia. Fasting serum levels of procollagen type I N-terminal propeptide (P1NP) and type I collagen C-terminal telopeptide (CTX; RatLaps) were measured by enzyme immunoassay (Immunodiagnosics Systems, Scottsdale, AZ) according to the manufacturer's protocol.

Cell Culture— $G_s\alpha$ (fl/fl) calvarial osteoblasts were harvested by serial collagenase digestion as described previously (47) and subjected to adenoviral infection with adeno-Cre or adeno- β -galactosidase (35). Cells were plated at 5×10^3 cells/cm² and induced to undergo osteogenic differentiation with ascorbic acid (50 μ g/ml) and β -glycerophosphate (10 mM). Rat PTH(1–34) (H-5460, Bachem, Dubendorf, Switzerland) was added to culture medium at 50 ng/ml for the first 6 h of every 48-h incubation cycle for 14 days.

Statistics—Statistical analyses were performed using a two-tailed Student's *t* test, and group differences were analyzed by two-way analysis of variance followed by post hoc Tukey's test. All values are expressed as means \pm S.E.

Results

To determine whether $G_s\alpha$ is required for the expansion of trabecular bone mediated by caPTH1R *in vivo*, we crossed $G_s\alpha^{OssxKO}$ mice with caPTH1R transgenic mice. At 1 week of age, histological analysis of proximal tibiae revealed that trabecular bone was nearly absent in $G_s\alpha^{OssxKO}$ mice but was greater than controls in caPTH1R mice (Fig. 1A). Skeletal preparations at 1 week of age demonstrated that healing calluses marked sites of rib fractures in $G_s\alpha^{OssxKO}$ but not caPTH1R mice (Fig. 1B). Double mutant mice (caPTH1R; $G_s\alpha^{OssxKO}$ mice) still exhibited rib fractures, and histological analysis revealed a paucity of trabecular bone that more closely resembled $G_s\alpha^{OssxKO}$ mice, although there were a few remaining fragments of trabecular bone (Fig. 1, A and B).

Constitutive expression of *Osx*-driven Cre recombinase throughout embryonic development resulted in severe osteoporosis at birth with the majority of $G_s\alpha^{OssxKO}$ mice dying by 3 weeks of age (34, 35), precluding analysis of $G_s\alpha$ conditional knock-out mice in adulthood. However, the osterix promoter-driven GFP::Cre fusion protein is regulated by a Tet-Off tetracycline transactivator (16). Doxycycline interferes with binding of tetracycline transactivator to its target and abolishes transcription of *Osx1*-GFP::Cre recombinase (48, 49). When doxycycline was administered in drinking water at 2 mg/ml to pregnant females from mating until 7 days after birth, caPTH1R; $G_s\alpha^{OssxKO}$ mice resembled caPTH1R mice with significantly greater trabecular bone mass, providing evidence that doxycycline prevented the deletion of $G_s\alpha$ (Fig. 1C). However, if doxycycline was withdrawn at day 7, then by day 21, caPTH1R; $G_s\alpha^{OssxKO}$ mice resembled $G_s\alpha^{OssxKO}$ mice by their marked reduction in trabecular bone mass (Fig. 1D). These results demonstrate that the caPTH1R mutant receptor requires expression of $G_s\alpha$ in osteoblasts to increase trabecular bone mass and suggest that $G_s\alpha$ expression in $G_s\alpha^{OssxKO}$ mice can be regulated by doxycycline administration.

Hong *et al.* (50) reported that high doses of doxycycline can lead to prolonged suppression of Cre expression even after withdrawal of doxycycline, whereas lower doses of doxycycline allow improved titration of Cre expression. We therefore tested doxycycline at a 200-fold lower dose (10 μ g/ml) in drinking water starting from conception. To determine whether Cre is expressed after withdrawal of doxycycline, we crossed $G_s\alpha^{OssxKO}$ mice to R26 reporter mice (37) in which a floxed stop cassette precedes the gene encoding β -galactosidase. Expression of Cre recombinase results in expression of β -galactosidase, which is detected by staining with X-Gal. Chen *et al.* (51) reported that the extraskeletal expression of *Osx1*-GFP::Cre is limited to the olfactory bulb, gastric, and intestinal epithelial cells; therefore we focused on X-Gal staining in bone. Following withdrawal of doxycycline at birth, we found abundant X-Gal staining of osteocytes and osteoblasts in *Osx1*-GFP::Cre⁺ mice, indicating Cre expression (Fig. 2A). In controls maintained on doxycycline until 6 weeks of age, X-Gal staining in the bone was significantly but not completely reduced (Fig. 2B). Despite incomplete suppression of Cre recombinase by doxycycline, the survival of P- $G_s\alpha^{OssxKO}$ mice, which in the absence of doxycycline do not survive to weaning, improved to 100% at 3 weeks of age (Fig. 2C).

To assess the effects of postnatal $G_s\alpha$ deletion, we administered 10 μ g/ml doxycycline throughout embryogenesis until birth (P0) and examined the skeleton at 6 weeks of age (Fig. 2D). Control mice did not express the Cre transgene; however, expression of the Cre transgene in wild-type mice did not significantly affect skeletal formation or bone mineral density, although Cre-expressing mice were slightly smaller (data not shown), consistent with previous reports of a transient decrease in body weight of *Osx*-Cre transgenic mice that resolves by 12 weeks of age (52). Histological analysis of P- $G_s\alpha^{OssxKO}$ mice at 6 weeks of age demonstrated low trabecular bone mass (Fig. 2E), and dual energy x-ray absorptiometry revealed reduced bone mineral density in the humerus (Fig. 2F). Serum calcium and phosphate levels did not differ between P- $G_s\alpha^{OssxKO}$ and con-

Low Bone Mass in Mice Lacking $G_s\alpha$ in the Postnatal Skeleton

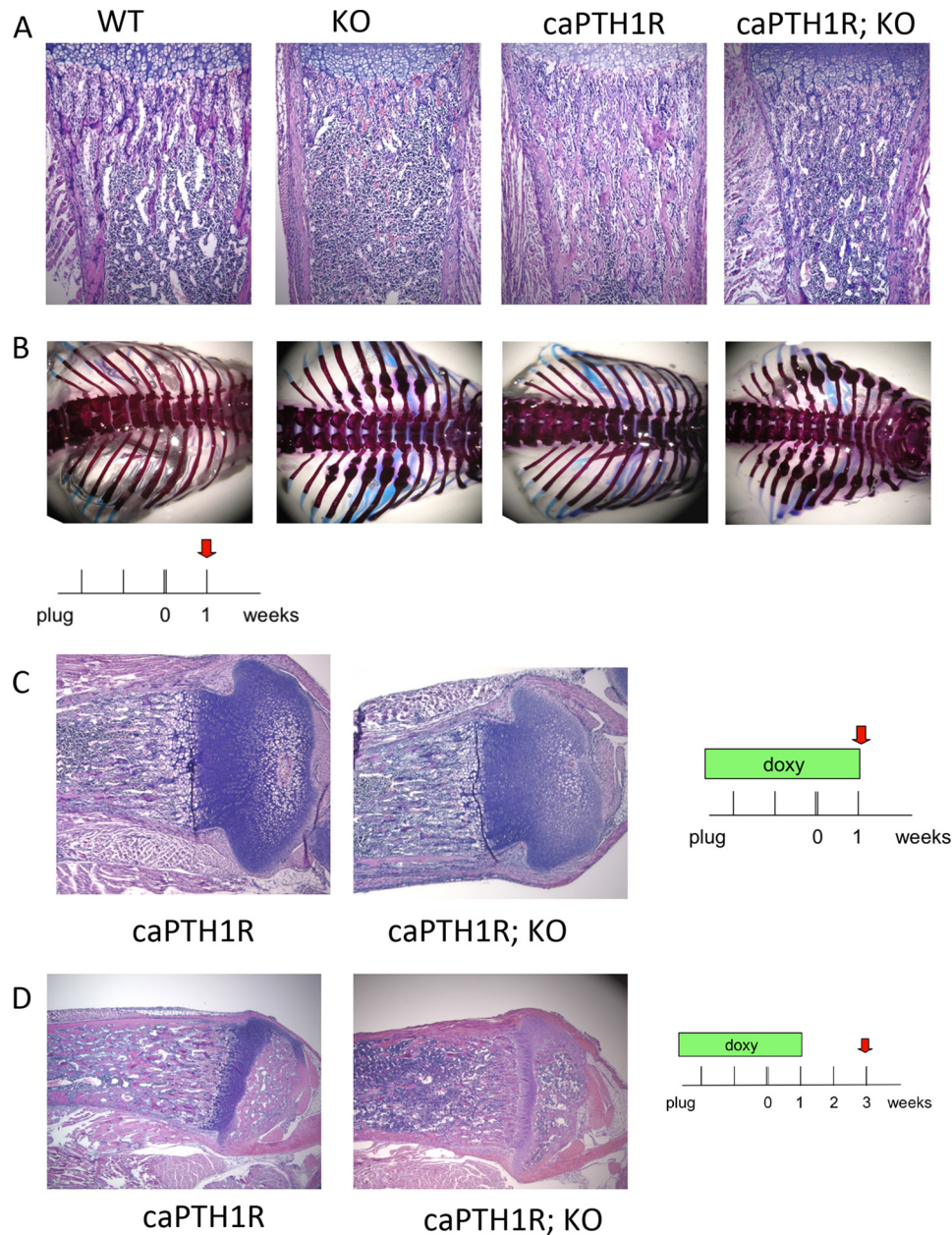


FIGURE 1. $G_s\alpha$ is required for increase of trabecular bone by constitutively active PTH1R. Hematoxylin- and eosin-stained sections of proximal tibiae (A) and skeletal preparations of rib cages of 7-day-old control (WT), $G_s\alpha^{\text{OsxKO}}$ (KO), caPTH1R, or double mutant (caPTH1R; KO) mice are shown. C, H&E-stained sections of proximal tibiae of caPTH1R or double mutant (caPTH1R; KO) mice treated with doxycycline (doxy) from plug until 1 week of age. D, H&E-stained sections of proximal tibiae of caPTH1R or double mutant (caPTH1R; KO) mice treated with doxycycline from plug until 1 week of age and analyzed at 3 weeks of age. Images are representative of at least three mice per genotype.

control littermates (data not shown). We have previously reported that *Gnas* mRNA levels are reduced by almost 90% in sorted *Osx1-GFP::Cre*⁺ cells of $G_s\alpha^{\text{OsxKO}}$ mice in which $G_s\alpha$ is deleted throughout embryogenesis (34). However, the yield of *Osx1-GFP::Cre*⁺ cells from mineralized adult bone is extremely low. We therefore prepared RNA from bone samples flushed of marrow and found that *Gnas* mRNA levels were reduced by 50% (Fig. 2G). Because $G_s\alpha$ is ubiquitously expressed, the remaining *Gnas* mRNA detected was likely largely expressed in non-osteoblast lineage cells.

As another approach to determine the effectiveness of $G_s\alpha$ deletion, we examined expression of sclerostin. Sclerostin is an inhibitor of canonical Wnt signaling that is suppressed by PTH.

Constitutive ablation of $G_s\alpha$ in the osteoblast lineage up-regulates *Sost*, the gene encoding sclerostin (35). We therefore examined *Sost* mRNA and sclerostin protein levels in P- $G_s\alpha^{\text{OsxKO}}$ mice. *Sost* mRNA increased >15-fold in bones of female P- $G_s\alpha^{\text{OsxKO}}$ mice (Fig. 2H). Immunohistochemical analysis for sclerostin protein also revealed a marked increase in sclerostin expression in P- $G_s\alpha^{\text{OsxKO}}$ osteocytes (Fig. 2I), suggesting deletion of $G_s\alpha$ with high efficiency from the osteoblast lineage.

To examine the role of $G_s\alpha$ in the anabolic response to PTH, control and P- $G_s\alpha^{\text{OsxKO}}$ mice were injected with once daily PTH(1–34) at 80 $\mu\text{g}/\text{kg}/\text{day}$ beginning at 8 weeks of age for 4 weeks (Fig. 3A). In vehicle (PBS)-treated mice, histological

Low Bone Mass in Mice Lacking $G_s\alpha$ in the Postnatal Skeleton

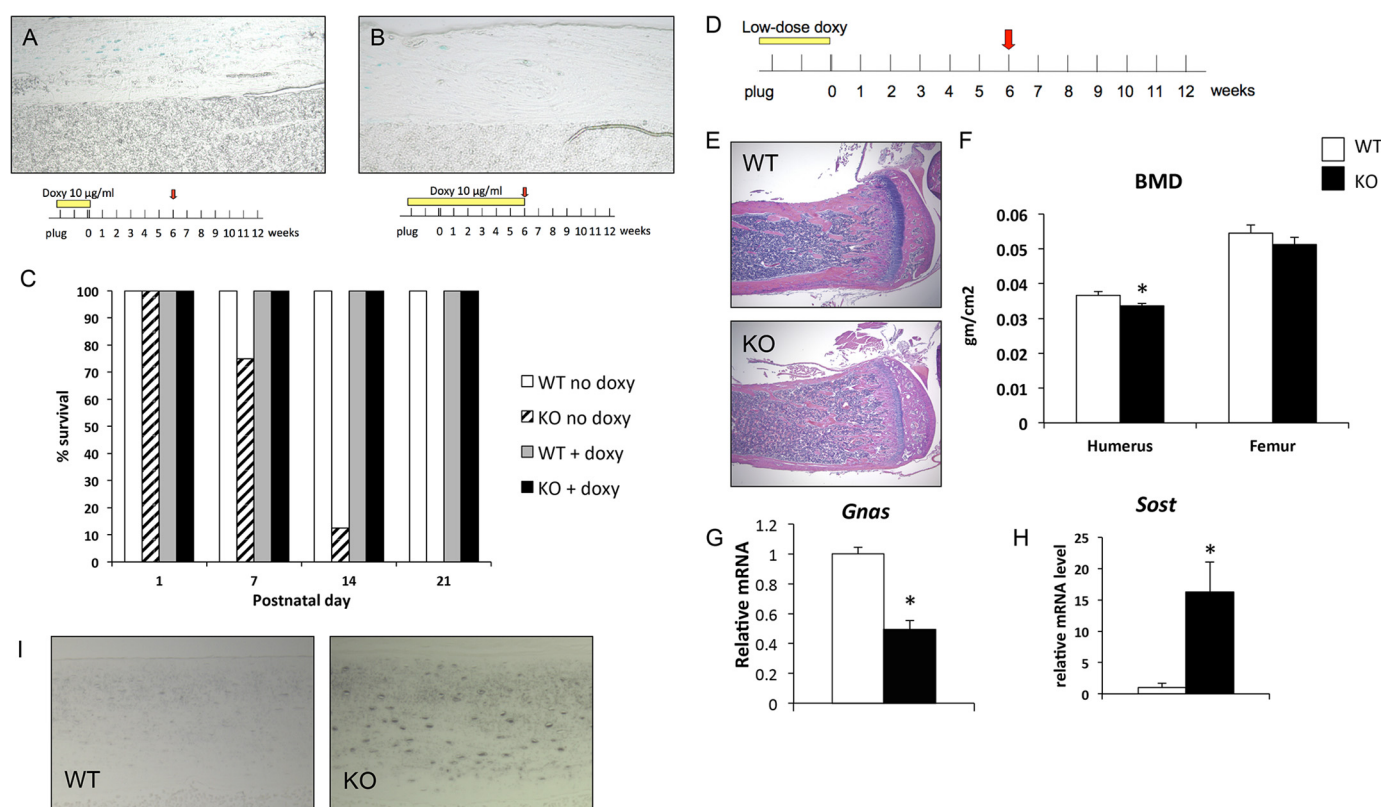


FIGURE 2. Postnatal deletion of $G_s\alpha$ leads to osteopenia and increased sclerostin expression. *A*, X-Gal staining for β -galactosidase activity in 6-week-old $G_s\alpha^{OxskKO}$ mice treated with doxycycline (Doxy) from plug until delivery ($100\times$ magnification). *B*, X-Gal staining of 6-week-old P- $G_s\alpha^{OxskKO}$ mice treated with doxycycline until 6 weeks of age ($100\times$). *C*, survival frequency in control (WT no doxy; white bar; $n = 18$) and $G_s\alpha^{OxskKO}$ (KO no doxy; hatched bar; $n = 8$) mice without doxycycline treatment or in control (WT + doxy; gray bar; $n = 7$) or P- $G_s\alpha^{OxskKO}$ mice (KO + doxy; black bar; $n = 10$) on $10\ \mu\text{g/ml}$ doxycycline from plug until birth. *D*, pregnant dams were administered $10\ \mu\text{g/ml}$ doxycycline in drinking water from plug until delivery. The resulting mice were analyzed at 6 weeks of age. *E*, H&E-stained sections of proximal tibia from female 6-week-old mice treated with $10\ \mu\text{g/ml}$ doxycycline until birth. *F*, bone mineral density (BMD) is significantly reduced in the humerus of P- $G_s\alpha^{OxskKO}$ mice. *gm*, gram. *G*, *Gnas* mRNA levels in femurs of WT and P- $G_s\alpha^{OxskKO}$ mice at 6 weeks. *H*, *Sost* mRNA levels in calvariae of 6-week-old mice. *I*, sclerostin immunostaining in cortical bone of WT and P- $G_s\alpha^{OxskKO}$ tibiae at 6 weeks of age. $n = 5$, WT; $n = 6$, P- $G_s\alpha^{OxskKO}$. *, $p < 0.05$. Error bars represent S.E.

analysis of the proximal humerus (Fig. 3*B*) and μCT analysis of distal femur trabecular bone (Fig. 3*C*) revealed low trabecular bone mass in P- $G_s\alpha^{OxskKO}$ male and female mice compared with controls. In females, PTH treatment increased BV/TV and Tb.N in WT compared with vehicle-treated mice, but this was not observed in P- $G_s\alpha^{OxskKO}$ mice where PTH treatment instead decreased Tb.N (Fig. 3, *D* and *E*). In males, PTH did not increase BV/TV or Tb.N in either WT or P- $G_s\alpha^{OxskKO}$ mice (Fig. 3, *D* and *E*). Trabecular thickness was significantly greater in PTH-treated WT and P- $G_s\alpha^{OxskKO}$ mice of both genders (Fig. 3*F*), and trabecular separation was increased in PTH-treated male and female P- $G_s\alpha^{OxskKO}$ mice as compared with WT controls (Fig. 3*G*). Cortical thickness was reduced in both male and female P- $G_s\alpha^{OxskKO}$ mice compared with WT controls; PTH treatment had no effect on this parameter (Fig. 4, *A* and *B*). Serum levels of P1NP, a marker of bone formation, did not differ in female mice, whereas in males P1NP was lower in PBS-treated P- $G_s\alpha^{OxskKO}$ mice than in WT, but PTH did not have any significant effect (Fig. 4*C*). In summary, in both male and female P- $G_s\alpha^{OxskKO}$ mice, PTH failed to increase trabecular bone volume or cortical thickness but did enhance trabecular thickness. In addition, PTH increased trabecular spacing in P- $G_s\alpha^{OxskKO}$ but not control mice.

Histomorphometric analysis of distal femora from male mice confirmed that BV/TV and trabecular number were lower in

PBS-treated P- $G_s\alpha^{OxskKO}$ compared with WT mice and that PTH treatment had no effect on either of these parameters (Table 1). Again, PTH increased trabecular thickness in WT and P- $G_s\alpha^{OxskKO}$ mice; no significant change in trabecular separation was observed. PTH treatment increased both osteoblast surface and osteoblast numbers in control mice and, surprisingly, in P- $G_s\alpha^{OxskKO}$ male mice. Bone formation rate as assessed by double calcein labeling was also greater in both control and P- $G_s\alpha^{OxskKO}$ male mice treated with PTH. The failure of intermittent PTH to increase bone volume in P- $G_s\alpha^{OxskKO}$ mice despite increased osteoblast numbers and bone formation rate could potentially be explained by high osteoclast activity. However, PTH treatment did not significantly alter osteoclast surface in either WT or KO mice (Table 1). There were no differences in serum levels of CTX, a marker of bone resorption, in either female or male mice (Fig. 4*D*).

To determine whether the effects of PTH on osteoblast numbers and bone formation rate in P- $G_s\alpha^{OxskKO}$ mice were mediated by direct action of PTH on osteoblasts, we isolated calvarial osteoblasts from mice with two floxed alleles of $G_s\alpha$. Infection of $G_s\alpha(\text{fl/fl})$ calvarial osteoblasts *in vitro* with adenovirus encoding Cre recombinase leads to efficient ($>90\%$) deletion of $G_s\alpha$ (35). We treated $G_s\alpha(\text{fl/fl})$ calvarial osteoblasts infected with Cre recombinase or β -gal control and then cul-

Low Bone Mass in Mice Lacking $G_s\alpha$ in the Postnatal Skeleton

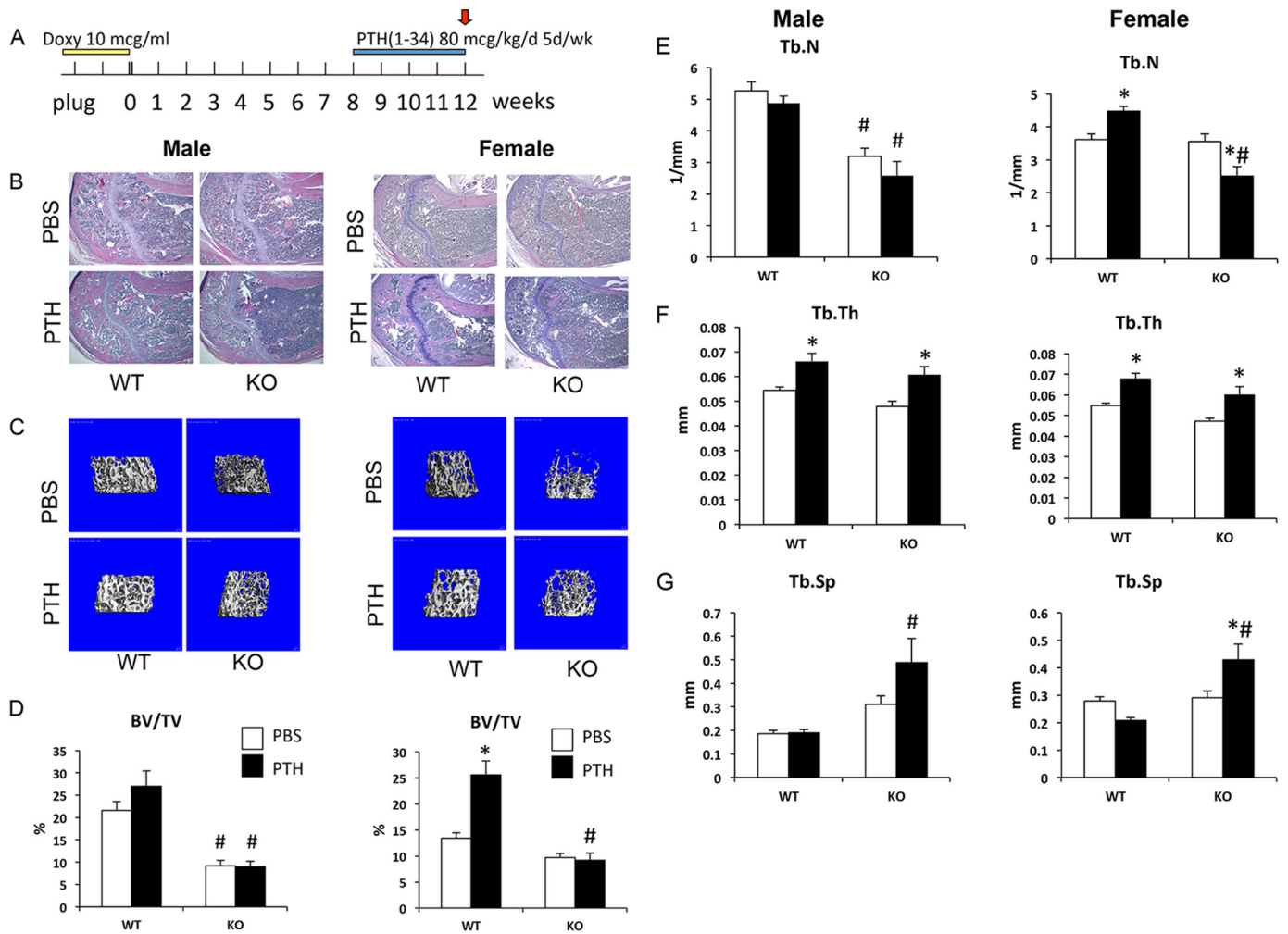


FIGURE 3. Intermittent PTH does not increase trabecular bone mass in P- $G_s\alpha^{OsxKO}$ male and female mice. *A*, mice were treated with 10 μg (mcg)/ml doxycycline from plug until delivery. At 8 weeks of age, control (WT) and P- $G_s\alpha^{OsxKO}$ (KO) mice were injected with 80 $\mu\text{g}/\text{kg}/\text{day}$ (d) PTH(1–34) or PBS 5 days/week (wk). H&E-stained sections of proximal humerus (*B*), μCT analysis of distal femur trabecular bone (*C*), BV/TV (*D*), Tb.N (*E*), Tb.Th (*F*), and Tb.Sp (*G*) of male (*left*) and female (*right*) mice are shown. $n = 6–9$ for each group of male mice, and $n = 5–8$ for each group of female mice. *, $p < 0.05$ versus respective PBS control; #, $p < 0.05$ versus respective WT control. Error bars represent S.E.

tured cells under osteogenic conditions with PTH or PBS for 6 h of every 48 h to stimulate osteoblast differentiation (53). In control osteoblasts, PTH increased mineralized nodule formation after 14 days, and as reported previously, deletion of $G_s\alpha$ led to markedly enhanced mineralization (35). Treatment with PTH further increased mineralized nodule formation by $G_s\alpha$ -deficient osteoblasts (Fig. 5, *A* and *B*). Mineralization can be increased by increased cell density. However, cell numbers were increased only transiently at day 3 in PTH-treated control osteoblasts (Fig. 5*C*). Examination of expression of markers of osteogenic differentiation confirmed that PTH treatment of $G_s\alpha$ -deficient osteoblasts significantly increased expression of a range of osteoblast marker genes including *Osx*, *Col1a1*, *Opn*, and *Bglap* as compared with PTH-treated control osteoblasts (Fig. 5*D*). This provides additional evidence that PTH can stimulate osteogenic differentiation in $G_s\alpha$ -deficient osteoblasts.

In addition to the $G_s\alpha$ -linked adenylyl cyclase-PKA signaling pathway, PTH is known to activate the G_q/G_{11} -linked PLC-PKC signaling pathway. PLC-defective mutant (D/D) mice express only a mutated PTH1R that activates adenylyl cyclase normally but cannot activate PLC (39). To determine whether

PLC signaling pathway via the PTH1R plays a role in bone anabolic action of PTH, we administered intermittent PTH to both PTH1R WT and D/D mice. Although a lowered bone mass was previously noted in growing tibiae of D/D mice at 6 and 10 weeks of age, at 16 weeks neither the tibia (determined by histomorphometry) nor the femur (examined by μCT) of D/D mice exhibited a significantly lower bone mass at baseline (Fig. 6 and Table 2). Intermittent PTH increased trabecular bone volume in the primary spongiosa in both WT and D/D mice; this area was excluded from standard measurement of histomorphometry (Fig. 6, *A* and *B*). Histomorphometry revealed no changes in bone architecture parameters (BV/TV, Tb.Th, and Tb.N) in the areas measured (Table 2). However, parameters of bone formation including mineral apposition rate, bone formation rate, bone volume and tissue volume, osteoid surface, osteoblast surface, and osteoblast number were increased by intermittent PTH in both WT and D/D mice (Table 2). In L5 vertebrae, as measured by μCT , PTH increased trabecular bone volume only in WT, but not D/D, mice (Fig. 6*C*). Trabecular number was not significantly altered by PTH treatment in either WT or D/D mice (Fig. 6*D*). PTH increased trabecular

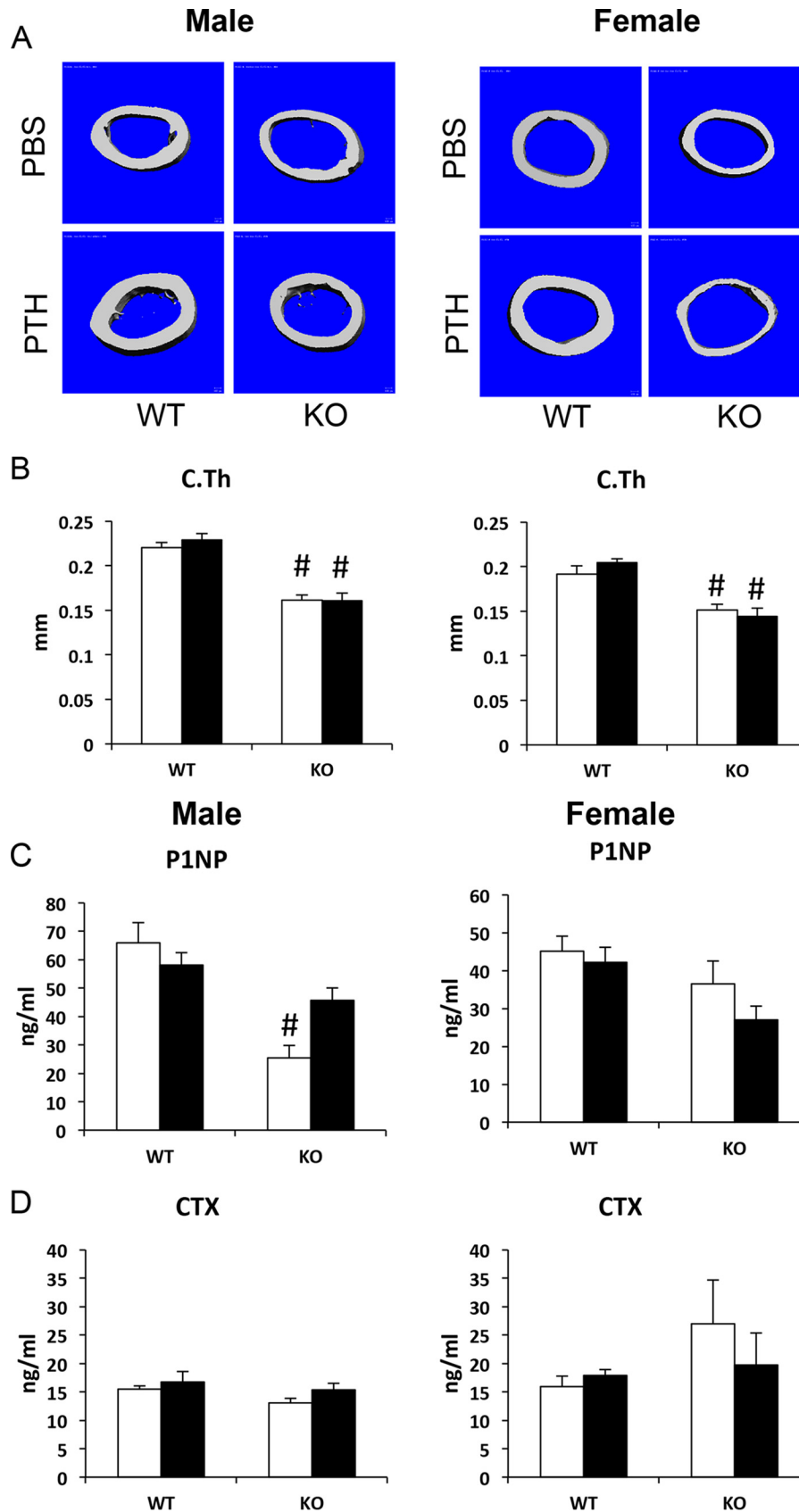


FIGURE 4. Cortical thickness is decreased in P- $G_s\alpha^{OxKO}$ male and female mice. μ CT analysis of femoral midshaft cortical bone (A) and cortical thickness (C.Th) in WT and P- $G_s\alpha^{OxKO}$ (KO) male (left) and female (right) mice treated with PBS and PTH is shown. $n = 6-9$ for each group of male mice, and $n = 5-8$ for each group of female mice. Serum levels of P1NP (C) and CTX (D) from male and female WT and P- $G_s\alpha^{OxKO}$ mice treated with PBS and PTH are shown. $n = 8-11$ for each group of male mice, and $n = 6-9$ for each group of female mice. *, $p < 0.05$ versus respective PBS control; #, $p < 0.05$ versus respective WT control. Error bars represent S.E.

Low Bone Mass in Mice Lacking $G_s\alpha$ in the Postnatal Skeleton

TABLE 1

Histomorphometry of 12-week-old control (WT) or P- $G_s\alpha^{OxskKO}$ (KO) tibiae with intermittent PTH or vehicle for 4 weeks

Values are mean \pm S.E. with $n = 6-9$ mice for each group. BFR, bone formation rate; BS, bone surface; MS, mineralizing surface; MAR, mineral apposition rate; Ob.S, osteoblast surface; N.Ob/B.Pm, number of osteoblasts per bone perimeter; O.Th, osteoid thickness; OS, osteoid surface; Os.S, osteoclast surface; N.Oc/B.Pm, number of osteoclasts per bone perimeter.

Parameters	WT		KO	
	PBS ($n = 8$)	PTH ($n = 9$)	PBS ($n = 6$)	PTH ($n = 6$)
BV/TV (%)	15.50 \pm 1.93	18.96 \pm 2.27	5.22 \pm 0.83 ^a	5.48 \pm 1.47 ^a
Tb.Th (μm)	37.84 \pm 1.79	48.98 \pm 2.38 ^b	28.62 \pm 1.29	37.29 \pm 3.24 ^{a,b}
Tb.N (/mm)	4.00 \pm 0.35	3.78 \pm 0.31	1.79 \pm 0.23 ^a	1.56 \pm 0.41 ^a
Tb.Sp (μm)	229.57 \pm 30.75	232.41 \pm 27.59	576.35 \pm 75.42	1324.96 \pm 622.91
MS/BS (%)	22.50 \pm 4.22	30.61 \pm 2.22	27.68 \pm 1.60	37.30 \pm 5.59 ^a
MAR ($\mu\text{m}/\text{day}$)	1.57 \pm 0.16	3.00 \pm 0.26 ^b	1.21 \pm 0.34	1.86 \pm 0.07 ^a
BFR/BS ($\mu\text{m}^3/\mu\text{m}^2/\text{day}$)	0.35 \pm 0.08	0.93 \pm 0.12 ^b	0.33 \pm 0.09	0.70 \pm 0.11 ^b
Ob.S/BS (%)	6.53 \pm 1.30	12.37 \pm 1.67 ^b	1.21 \pm 0.77	8.22 \pm 2.27 ^b
N.Ob/B.Pm (/mm)	4.08 \pm 0.89	8.19 \pm 1.35 ^b	0.76 \pm 0.49	5.35 \pm 1.56 ^b
OS/BS (%)	2.05 \pm 0.64	6.49 \pm 1.91	0.16 \pm 0.16	2.91 \pm 1.05 ^b
O.Th (μm)	0.60 \pm 0.11	0.87 \pm 0.22	0.05 \pm 0.05	0.48 \pm 0.16
Oc.S/BS (%)	4.97 \pm 0.71	5.31 \pm 0.32	5.03 \pm 0.73	6.67 \pm 0.60
N.Oc/B.Pm (/mm)	2.27 \pm 0.33	2.17 \pm 0.13	2.86 \pm 0.47	3.34 \pm 0.35

^a $p < 0.05$ versus respective WT control.

^b $p < 0.05$ versus respective PBS control.

thickness in both WT and D/D mice (Fig. 6E) but had no effect on trabecular separation (Fig. 6F).

We measured serum P1NP as a bone formation marker and serum CTX as a bone resorption marker (Fig. 6, G and H). Both P1NP and CTX were significantly increased by PTH in WT and D/D mice; the level of P1NP in PTH-treated D/D mice was lower than that of PTH-treated WT mice (Fig. 6G).

Discussion

We have found that $G_s\alpha$ signaling in the osteoblast lineage is important not only for embryonic skeletal development but also for adult skeletal homeostasis. Furthermore, we have demonstrated that $G_s\alpha$ is a downstream mediator of anabolic PTH signaling *in vivo* by two approaches. First, we crossed mice lacking $G_s\alpha$ in osteoblasts to mice expressing caPTH1R in osteoblasts and found that the postnatal absence of $G_s\alpha$ markedly attenuates the ability of caPTH1R to increase trabecular bone. Second, we administered intermittent PTH to adult mice lacking $G_s\alpha$ in osteoblasts and found that in the absence of $G_s\alpha$ the anabolic actions of intermittent PTH on trabecular bone are blunted *in vivo*.

Mice with postnatal ablation of $G_s\alpha$ in osteoblast progenitors (P- $G_s\alpha^{OxskKO}$ mice) have severe osteoporosis affecting both trabecular and cortical bone. Osteoclast surface and CTX levels are not elevated, indicating that their low bone mass is not due to enhanced bone resorption. These findings are consistent with our previous studies demonstrating failure of bone formation in mice with deletion of $G_s\alpha$ in osteoprogenitors throughout embryonic development (35).

PTH increased osteoblast numbers and bone formation rate in P- $G_s\alpha^{OxskKO}$ mice, a paradoxical finding because PTH failed to increase overall bone mass in those mice. A proportionally greater increase in resorption in response to PTH by P- $G_s\alpha^{OxskKO}$ mice would be one explanation; however, there was no significant increase in osteoclast surface, CTX levels, or trabecular separation in P- $G_s\alpha^{OxskKO}$ mice treated with intermittent PTH, and trabecular thickness was increased. An alternative explanation is that by 8 weeks of age when anabolic PTH was started P- $G_s\alpha^{OxskKO}$ mice have insufficient trabecular bone surface on which new bone can be formed; studies are now

underway to begin PTH treatment earlier before bone loss has progressed to such an advanced degree in P- $G_s\alpha^{OxskKO}$ mice. Finally, in cultured osteoblasts, PTH can maximally activate PKA at concentrations significantly lower than required to increase total cAMP levels, suggesting that only a fraction of the total cAMP that can be generated by PTH stimulation is required for PKA activation (54). It is also important to note that $G_s\alpha$ -mediated PTH1R signaling in other tissues such as the kidney is presumably preserved. Careful analysis of postnatal extraskeletal *Osx-Cre* expression by Chen *et al.* (51) revealed that although *Osx-Cre* targets cells in the olfactory bulb, gastric, and intestinal epithelia there is no expression in the kidney, liver, or other organs. Therefore indirect effects of PTH, for example on systemic mineral metabolism, may also influence skeletal homeostasis. However, we found that PTH does have direct effects in osteoblasts that are altered by the removal of $G_s\alpha$.

The mechanisms by which intermittent PTH stimulates osteoblast differentiation and function are incompletely understood. Because PTH treatment has a positive effect on osteoblast surface in $G_s\alpha$ -deficient mice, it is likely that PTH also stimulates signaling pathways downstream of PTH1R independent of $G_s\alpha$. These may include pathways activated by other PTH1R-coupled G proteins including G_q/G_{11} and G_{12}/G_{13} (29, 30). We found that although intermittent PTH in older mice did not significantly increase trabecular bone volume in long bones of either WT or D/D mice within the time frame of this experiment it did significantly increase almost all parameters of bone formation in both WT and D/D mice. Our data suggest that PLC signaling through the PTH1R is therefore not required for PTH-stimulated bone turnover in mature mice. However, our findings do not rule out the possibility that in the absence of $G_s\alpha$ activation of $G_{q/11}$ may mediate some of the anabolic effects of PTH.

In addition to PTH1R-coupled G proteins, β -arrestins have also been implicated in the anabolic response to PTH, and the anabolic effect of PTH is blunted in the absence of β -arrestin2 (55). Initially identified based on their roles in G protein-coupled receptor desensitization, growing evidence suggests that

Low Bone Mass in Mice Lacking $G_s\alpha$ in the Postnatal Skeleton

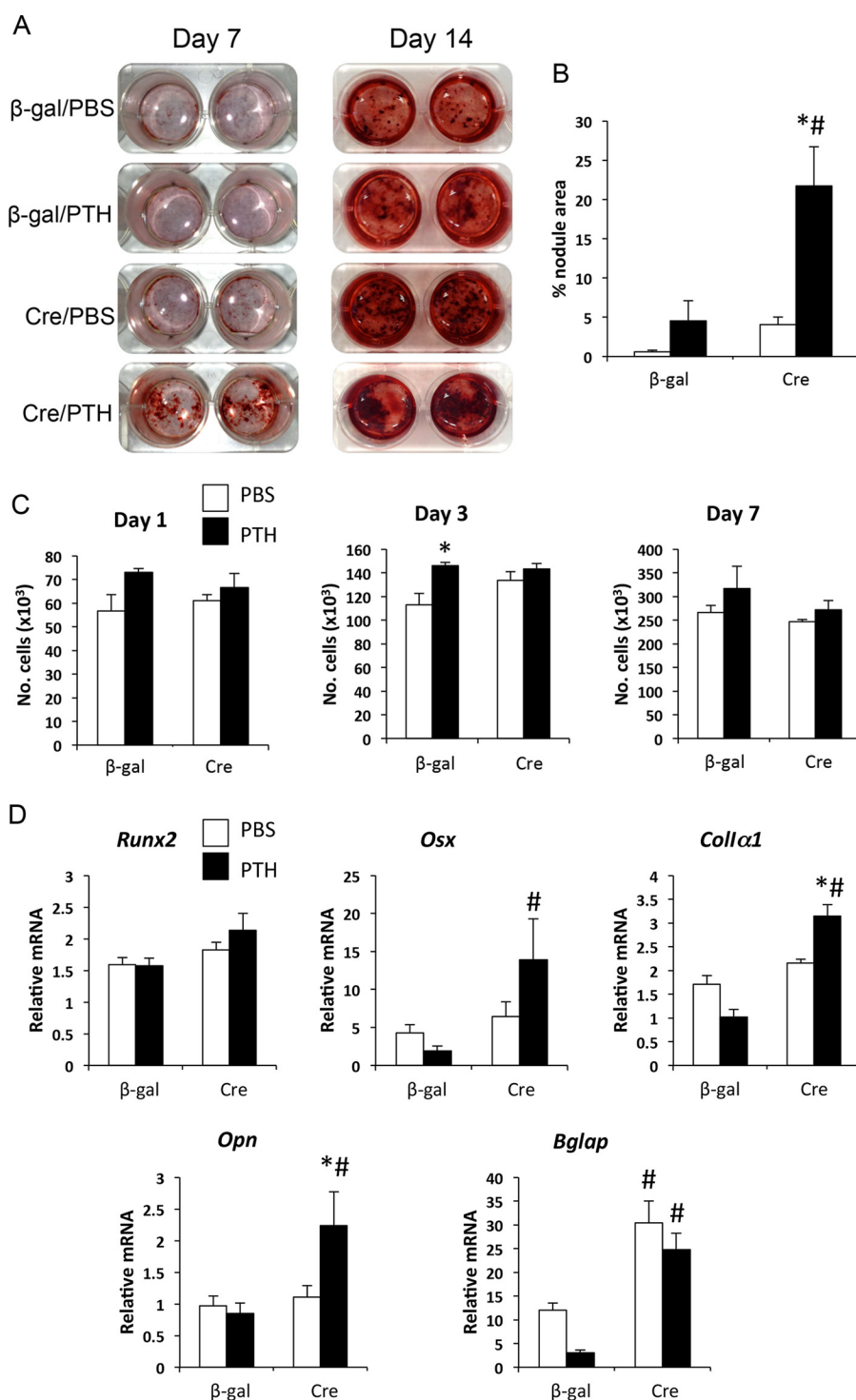


FIGURE 5. PTH enhances osteogenic differentiation of $G_s\alpha$ -deficient osteoblasts. *A*, Alizarin red staining of $G_s\alpha$ (fl/fl) calvarial osteoblasts infected with adeno- β -gal (control) or adeno-Cre, then treated with PBS or PTH for 6 h of every 48 h, and subjected to osteogenic differentiation for 7 and 14 days. *B*, quantitation of mineralized nodule area at day 14. *C*, numbers of cells per well of $G_s\alpha$ (fl/fl) calvarial osteoblasts treated with adeno- β -gal or adeno-Cre and then with PBS or PTH. *n* = 3 experiments. *D*, mRNA expression levels of *Runx2*, *Osx*, *Collα1*, *Opn*, and *Bglap* at day 7 in cells described above. Mean results from three replicate experiments are shown. *, $p < 0.05$ versus respective PBS control; #, $p < 0.05$ versus respective WT control. Error bars represent S.E.

β -arrestins can themselves mediate signaling downstream of G protein-coupled receptors. Activation of PTH1R by PTH stimulates both $G_s\alpha$ - and β -arrestin-mediated activation of mitogen-activated protein kinases ERK1/2; although $G_s\alpha$ activation leads to an early increase in ERK activity, β -arrestins contribute

to a later, sustained activation of ERK1/2 (32). A modified PTH peptide that attenuates $G_s\alpha$ -dependent signaling while stimulating β -arrestin-dependent signaling (PTH- β arr) (32) can still increase bone mass as well as bone formation rate and osteoblast surface in a β -arrestin2-dependent manner (56), although

Low Bone Mass in Mice Lacking $G_s\alpha$ in the Postnatal Skeleton

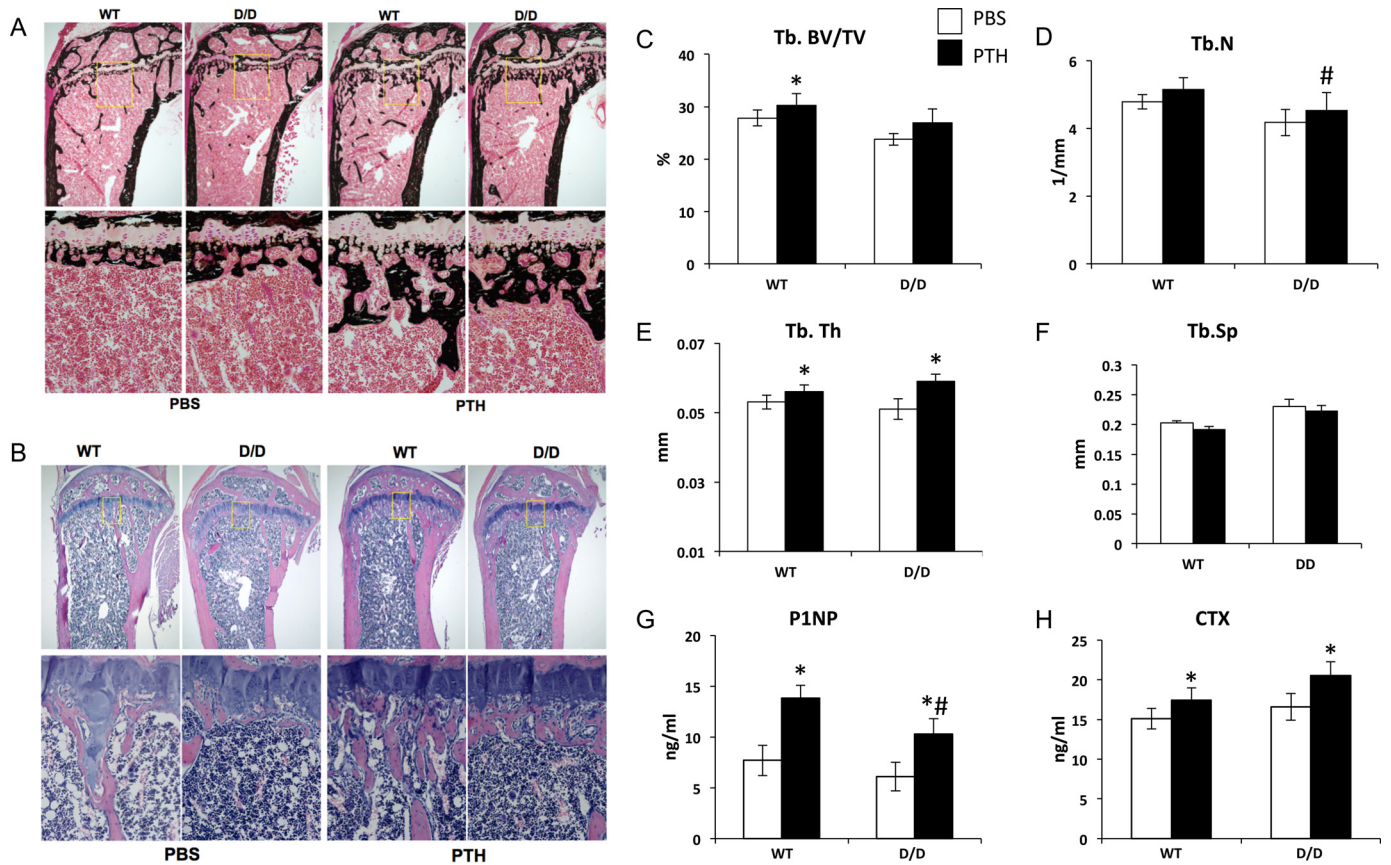


FIGURE 6. Intermittent PTH increases bone formation in DSEL mice. von Kossa-stained plastic sections (A) and H&E stained paraffin sections (B) from proximal tibiae of 16-week old WT and DSEL (D/D) mice treated with vehicle (VEH) or intermittent PTH (80 $\mu\text{g}/\text{kg}/\text{day}$) from 12 weeks of age. $n = 7-9$ for each group. C-F, μCT analysis of 16-week-old L5 vertebrae from WT and DSEL (D/D) mice treated with vehicle (PBS) or intermittent PTH (80 $\mu\text{g}/\text{kg}/\text{day}$) for the last 4 weeks. Tb.BV/TV (%) (C), Tb.N (1/mm) (D), Tb.Th (mm) (E), and Tb.Sp (1/mm³) (F) were measured in eight to nine animals of each group. Serum P1NP (G) and CTX (H) were measured in 16-week-old WT and DSEL (D/D) mice treated with vehicle (VEH) or intermittent PTH (80 $\mu\text{g}/\text{kg}/\text{day}$) for the last 4 weeks. $n = 8$ per group. *, $p < 0.05$ versus respective PBS control; #, $p < 0.05$ versus respective WT control. Error bars represent S.E.

TABLE 2

Histomorphometry of 16-week-old control (WT) or D/D tibiae with intermittent PTH or vehicle for 4 weeks

Values are mean \pm S.E. with $n = 7-9$ mice for each group. BFR, bone formation rate; BS, bone surface; MS, mineralizing surface; MAR, mineral apposition rate; Ob.S, osteoblast surface; N.Ob/B.Pm, number of osteoblasts per bone perimeter; O.Th, osteoid thickness; OS, osteoid surface; Os.S, osteoclast surface; N.Oc/B.Pm, number of osteoclasts per bone perimeter.

Parameters	WT		D/D	
	PBS ($n = 8$)	PTH ($n = 8$)	PBS ($n = 7$)	PTH ($n = 9$)
BV/TV (%)	4.84 \pm 0.80	5.97 \pm 1.04	3.72 \pm 0.54	5.10 \pm 0.91
Tb.Th (μm)	33.62 \pm 3.28	35.57 \pm 2.34	28.73 \pm 1.63	32.42 \pm 1.80
Tb.N (1/mm)	1.44 \pm 0.19	1.61 \pm 0.24	1.27 \pm 0.15	1.54 \pm 0.23
Tb.Sp (μm)	759 \pm 109	708 \pm 133	823 \pm 94	839 \pm 228
MS/BS (%)	21.27 \pm 1.43	31.54 \pm 1.66 ^a	24.97 \pm 1.28	25.70 \pm 2.24
MAR ($\mu\text{m}/\text{day}$)	1.90 \pm 0.14	2.34 \pm 0.12 ^a	1.56 \pm 0.21	2.52 \pm 0.13 ^a
BFR/BS ($\mu\text{m}^3/\mu\text{m}^2/\text{year}$)	147 \pm 14	270 \pm 23 ^a	141 \pm 20	238 \pm 26 ^a
Ob.S/BS (%)	14.25 \pm 2.77	29.45 \pm 2.15 ^a	17.97 \pm 3.59	31.47 \pm 2.77 ^a
N.Ob/B.Pm (1/mm)	11.47 \pm 1.95	23.64 \pm 1.75 ^a	14.09 \pm 3.05	22.87 \pm 1.67 ^a
OS/BS (%)	4.36 \pm 1.12	19.51 \pm 1.86 ^a	7.45 \pm 2.35	14.41 \pm 1.51 ^a
O.Th (μm)	2.31 \pm 0.30	2.83 \pm 0.18	2.48 \pm 0.12	2.73 \pm 0.15
Oc.S/BS (%)	2.36 \pm 0.69	5.24 \pm 0.97 ^a	3.39 \pm 0.64	5.82 \pm 1.04
N.Oc/B.Pm (1/mm)	0.94 \pm 0.28	1.97 \pm 0.36 ^a	1.37 \pm 0.29	2.55 \pm 0.61

^a $p < 0.05$ versus respective PBS control.

effects mediated by stimulation of endogenous PTH secretion were not ruled out. Studies are now underway to address the role of non- $G_s\alpha$ -mediated signaling pathways downstream of PTH1R.

Author Contributions—J. Y. W. conceived and coordinated the study and wrote the paper. J. Y. W., G. N., and E. S. designed, performed, and analyzed the experiments shown in Fig. 1. J. Y. W. and P. A. designed, performed, and analyzed the experiments shown in Fig. 2. P. S. and R. C. designed, performed, and analyzed the experiments shown in Figs. 3 and 4. I. J. P. and N. A. S. designed, performed, and analyzed the experiments shown in Table 1. H. S. designed, performed, and analyzed the experiments shown in Fig. 5. J. G. and H. M. K. designed, performed, and analyzed the experiments shown in Table 2. M. C. and L. S. W. generated the $G_s\alpha$ -floxed mice and contributed to experimental design and data interpretation. All authors reviewed the results and approved the final version of the manuscript.

Acknowledgments—We thank Dr. Andrew McMahon for providing *Osx1-GFP::Cre* mice and the Massachusetts General Hospital Center for Comparative Medicine and Stanford Veterinary Services Center staff for care of the animals.

References

- Burge, R., Dawson-Hughes, B., Solomon, D. H., Wong, J. B., King, A., and Tosteson, A. (2007) Incidence and economic burden of osteoporosis-related fractures in the United States, 2005–2025. *J. Bone Miner. Res.* **22**, 465–475
- Raisz, L. G. (2005) Pathogenesis of osteoporosis: concepts, conflicts, and prospects. *J. Clin. Investig.* **115**, 3318–3325

3. Neer, R. M., Arnaud, C. D., Zanchetta, J. R., Prince, R., Gaich, G. A., Reginster, J. Y., Hodsman, A. B., Eriksen, E. F., Ish-Shalom, S., Genant, H. K., Wang, O., and Mitlak, B. H. (2001) Effect of parathyroid hormone (1–34) on fractures and bone mineral density in postmenopausal women with osteoporosis. *N. Engl. J. Med.* **344**, 1434–1441
4. Bellido, T., Ali, A. A., Plotkin, L. I., Fu, Q., Gubrij, I., Roberson, P. K., Weinstein, R. S., O'Brien, C. A., Manolagas, S. C., and Jilka, R. L. (2003) Proteasomal degradation of Runx2 shortens parathyroid hormone-induced anti-apoptotic signaling in osteoblasts. A putative explanation for why intermittent administration is needed for bone anabolism. *J. Biol. Chem.* **278**, 50259–50272
5. Dobnig, H., and Turner, R. T. (1997) The effects of programmed administration of human parathyroid hormone fragment (1–34) on bone histomorphometry and serum chemistry in rats. *Endocrinology* **138**, 4607–4612
6. Iida-Klein, A., Zhou, H., Lu, S. S., Levine, L. R., Ducayen-Knowles, M., Dempster, D. W., Nieves, J., and Lindsay, R. (2002) Anabolic action of parathyroid hormone is skeletal site specific at the tissue and cellular levels in mice. *J. Bone Miner. Res.* **17**, 808–816
7. Jilka, R. L. (2007) Molecular and cellular mechanisms of the anabolic effect of intermittent PTH. *Bone* **40**, 1434–1446
8. Jilka, R. L., O'Brien, C. A., Ali, A. A., Roberson, P. K., Weinstein, R. S., and Manolagas, S. C. (2009) Intermittent PTH stimulates periosteal bone formation by actions on post-mitotic preosteoblasts. *Bone* **44**, 275–286
9. Jilka, R. L., Weinstein, R. S., Bellido, T., Roberson, P., Parfitt, A. M., and Manolagas, S. C. (1999) Increased bone formation by prevention of osteoblast apoptosis with parathyroid hormone. *J. Clin. Investig.* **104**, 439–446
10. Kim, S. W., Pajevic, P. D., Selig, M., Barry, K. J., Yang, J. Y., Shin, C. S., Baek, W. Y., Kim, J. E., and Kronenberg, H. M. (2012) Intermittent parathyroid hormone administration converts quiescent lining cells to active osteoblasts. *J. Bone Miner. Res.* **27**, 2075–2084
11. Lindsay, R., Cosman, F., Zhou, H., Bostrom, M. P., Shen, V. W., Cruz, J. D., Nieves, J. W., and Dempster, D. W. (2006) A novel tetracycline labeling schedule for longitudinal evaluation of the short-term effects of anabolic therapy with a single iliac crest bone biopsy: early actions of teriparatide. *J. Bone Miner. Res.* **21**, 366–373
12. Li, X., Zhang, Y., Kang, H., Liu, W., Liu, P., Zhang, J., Harris, S. E., and Wu, D. (2005) Sclerostin binds to LRP5/6 and antagonizes canonical Wnt signaling. *J. Biol. Chem.* **280**, 19883–19887
13. Semenov, M., Tamai, K., and He, X. (2005) SOST is a ligand for LRP5/LRP6 and a Wnt signaling inhibitor. *J. Biol. Chem.* **280**, 26770–26775
14. Day, T. F., Guo, X., Garrett-Beal, L., and Yang, Y. (2005) Wnt/ β -catenin signaling in mesenchymal progenitors controls osteoblast and chondrocyte differentiation during vertebrate skeletogenesis. *Dev. Cell* **8**, 739–750
15. Hill, T. P., Später, D., Taketo, M. M., Birchmeier, W., and Hartmann, C. (2005) Canonical Wnt/ β -catenin signaling prevents osteoblasts from differentiating into chondrocytes. *Dev. Cell* **8**, 727–738
16. Rodda, S. J., and McMahon, A. P. (2006) Distinct roles for Hedgehog and canonical Wnt signaling in specification, differentiation and maintenance of osteoblast progenitors. *Development* **133**, 3231–3244
17. Balemans, W., Ebeling, M., Patel, N., Van Hul, E., Olson, P., Dioszegi, M., Lacza, C., Wuys, W., Van Den Ende, J., Willems, P., Paes-Alves, A. F., Hill, S., Bueno, M., Ramos, F. J., Tacconi, P., Dikkers, F. G., Stratakis, C., Lindpaintner, K., Vickery, B., Foerzler, D., and Van Hul, W. (2001) Increased bone density in sclerosteosis is due to the deficiency of a novel secreted protein (SOST). *Hum. Mol. Genet.* **10**, 537–543
18. Brunkow, M. E., Gardner, J. C., Van Ness, J., Paeper, B. W., Kovacevich, B. R., Proll, S., Skonier, J. E., Zhao, L., Sabo, P. J., Fu, Y., Alisch, R. S., Gillett, L., Colbert, T., Tacconi, P., Galas, D., Hamersma, H., Beighton, P., and Mulligan, J. (2001) Bone dysplasia sclerosteosis results from loss of the SOST gene product, a novel cystine knot-containing protein. *Am. J. Hum. Genet.* **68**, 577–589
19. McClung, M. R., Grauer, A., Boonen, S., Bolognese, M. A., Brown, J. P., Diez-Perez, A., Langdahl, B. L., Reginster, J. Y., Zanchetta, J. R., Wasserman, S. M., Katz, L., Maddox, J., Yang, Y. C., Libanati, C., and Bone, H. G. (2014) Romosozumab in postmenopausal women with low bone mineral density. *N. Engl. J. Med.* **370**, 412–420
20. Kedlaya, R., Veera, S., Horan, D. J., Moss, R. E., Ayturk, U. M., Jacobsen, C. M., Bowen, M. E., Paszty, C., Warman, M. L., and Robling, A. G. (2013) Sclerostin inhibition reverses skeletal fragility in an Lrp5-deficient mouse model of OPGG syndrome. *Sci. Transl. Med.* **5**, 211ra158
21. Sinder, B. P., Eddy, M. M., Ominsky, M. S., Caird, M. S., Marini, J. C., and Kozloff, K. M. (2013) Sclerostin antibody improves skeletal parameters in a *Brlt1*+/+ mouse model of osteogenesis imperfecta. *J. Bone Miner. Res.* **28**, 73–80
22. Pearman, A. T., Chou, W. Y., Bergman, K. D., Pulumati, M. R., and Partridge, N. C. (1996) Parathyroid hormone induces c-fos promoter activity in osteoblastic cells through phosphorylated cAMP response element (CRE)-binding protein binding to the major CRE. *J. Biol. Chem.* **271**, 25715–25721
23. Boguslawski, G., Hale, L. V., Yu, X. P., Miles, R. R., Onyia, J. E., Santerre, R. F., and Chandrasekhar, S. (2000) Activation of osteocalcin transcription involves interaction of protein kinase A- and protein kinase C-dependent pathways. *J. Biol. Chem.* **275**, 999–1006
24. Selvamurugan, N., Chou, W. Y., Pearman, A. T., Pulumati, M. R., and Partridge, N. C. (1998) Parathyroid hormone regulates the rat collagenase-3 promoter in osteoblastic cells through the cooperative interaction of the activator protein-1 site and the runt domain binding sequence. *J. Biol. Chem.* **273**, 10647–10657
25. Lee, S. K., and Lorenzo, J. A. (1999) Parathyroid hormone stimulates TRANCE and inhibits osteoprotegerin messenger ribonucleic acid expression in murine bone marrow cultures: correlation with osteoclast-like cell formation. *Endocrinology* **140**, 3552–3561
26. Calvi, L. M., Sims, N. A., Hunzelman, J. L., Knight, M. C., Giovannetti, A., Saxton, J. M., Kronenberg, H. M., Baron, R., and Schipani, E. (2001) Activated parathyroid hormone/parathyroid hormone-related protein receptor in osteoblastic cells differentially affects cortical and trabecular bone. *J. Clin. Investig.* **107**, 277–286
27. Schipani, E., Kruse, K., and Jüppner, H. (1995) A constitutively active mutant PTH-PTHrP receptor in Jansen-type metaphyseal chondrodysplasia. *Science* **268**, 98–100
28. Hsiao, E. C., Boudignon, B. M., Chang, W. C., Bencsik, M., Peng, J., Nguyen, T. D., Manalac, C., Halloran, B. P., Conklin, B. R., and Nissenson, R. A. (2008) Osteoblast expression of an engineered Gs-coupled receptor dramatically increases bone mass. *Proc. Natl. Acad. Sci. U.S.A.* **105**, 1209–1214
29. Abou-Samra, A. B., Jüppner, H., Force, T., Freeman, M. W., Kong, X. F., Schipani, E., Urena, P., Richards, J., Bonventre, J. V., Potts, J. T., Jr., Kronenberg, H. M., and Segre, G. V. (1992) Expression cloning of a common receptor for parathyroid hormone and parathyroid hormone-related peptide from rat osteoblast-like cells: a single receptor stimulates intracellular accumulation of both cAMP and inositol trisphosphates and increases intracellular free calcium. *Proc. Natl. Acad. Sci. U.S.A.* **89**, 2732–2736
30. Singh, A. T., Gilchrist, A., Voyno-Yasenetskaya, T., Radeff-Huang, J. M., and Stern, P. H. (2005) $G_{\alpha 12}/G_{\alpha 13}$ subunits of heterotrimeric G proteins mediate parathyroid hormone activation of phospholipase D in UMR-106 osteoblastic cells. *Endocrinology* **146**, 2171–2175
31. Guo, J., Liu, M., Yang, D., Bouxsein, M. L., Thomas, C. C., Schipani, E., Bringham, F. R., and Kronenberg, H. M. (2010) Phospholipase C signaling via the parathyroid hormone (PTH)/PTH-related peptide receptor is essential for normal bone responses to PTH. *Endocrinology* **151**, 3502–3513
32. Gesty-Palmer, D., Chen, M., Reiter, E., Ahn, S., Nelson, C. D., Wang, S., Eckhardt, A. E., Cowan, C. L., Spurney, R. F., Luttrell, L. M., and Lefkowitz, R. J. (2006) Distinct β -arrestin- and G protein-dependent pathways for parathyroid hormone receptor-stimulated ERK1/2 activation. *J. Biol. Chem.* **281**, 10856–10864
33. Sinha, P., Aarnisalo, P., Chubb, R., Ono, N., Fulzele, K., Selig, M., Saeed, H., Chen, M., Weinstein, L. S., Pajevic, P. D., Kronenberg, H. M., and Wu, J. Y. (2014) Loss of G_{α} early in the osteoblast lineage favors adipogenic differentiation of mesenchymal progenitors and committed osteoblast precursors. *J. Bone Miner. Res.* **29**, 2414–2426
34. Wu, J. Y., Purton, L. E., Rodda, S. J., Chen, M., Weinstein, L. S., McMahon, A. P., Scadden, D. T., and Kronenberg, H. M. (2008) Osteoblastic regulation of B lymphopoiesis is mediated by G_{α} -dependent signaling pathways. *Proc. Natl. Acad. Sci. U.S.A.* **105**, 16976–16981
35. Wu, J. Y., Aarnisalo, P., Bastepe, M., Sinha, P., Fulzele, K., Selig, M. K.,

Low Bone Mass in Mice Lacking $G_s\alpha$ in the Postnatal Skeleton

- Chen, M., Poulton, I. J., Purton, L. E., Sims, N. A., Weinstein, L. S., and Kronenberg, H. M. (2011) $G_s\alpha$ enhances commitment of mesenchymal progenitors to the osteoblast lineage but restrains osteoblast differentiation in mice. *J. Clin. Investig.* **121**, 3492–3504
36. Hsiao, E. C., Boudignon, B. M., Halloran, B. P., Nissenson, R. A., and Conklin, B. R. (2010) G_s G protein-coupled receptor signaling in osteoblasts elicits age-dependent effects on bone formation. *J. Bone Miner. Res.* **25**, 584–593
37. Soriano, P. (1999) Generalized lacZ expression with the ROSA26 Cre reporter strain. *Nat. Genet.* **21**, 70–71
38. Muzumdar, M. D., Tasic, B., Miyamichi, K., Li, L., and Luo, L. (2007) A global double-fluorescent Cre reporter mouse. *Genesis* **45**, 593–605
39. Guo, J., Chung, U. I., Kondo, H., Bringhurst, F. R., and Kronenberg, H. M. (2002) The PTH/PTHrP receptor can delay chondrocyte hypertrophy *in vivo* without activating phospholipase C. *Dev. Cell* **3**, 183–194
40. Dobreva, G., Chahrour, M., Dautzenberg, M., Chirivella, L., Kanzler, B., Fariñas, I., Karsenty, G., and Grosschedl, R. (2006) SATB2 is a multifunctional determinant of craniofacial patterning and osteoblast differentiation. *Cell* **125**, 971–986
41. Boussein, M. L., Boyd, S. K., Christiansen, B. A., Guldborg, R. E., Jepsen, K. J., and Müller, R. (2010) Guidelines for assessment of bone microstructure in rodents using micro-computed tomography. *J. Bone Miner. Res.* **25**, 1468–1486
42. Sims, N. A., Brennan, K., Spaliviero, J., Handelsman, D. J., and Seibel, M. J. (2006) Perinatal testosterone surge is required for normal adult bone size but not for normal bone remodeling. *Am. J. Physiol. Endocrinol. Metab.* **290**, E456–E462
43. Bastepe, M., Weinstein, L. S., Ogata, N., Kawaguchi, H., Jüppner, H., Kronenberg, H. M., and Chung, U. I. (2004) Stimulatory G protein directly regulates hypertrophic differentiation of growth plate cartilage *in vivo*. *Proc. Natl. Acad. Sci. U.S.A.* **101**, 14794–14799
44. Kenner, L., Hoebertz, A., Beil, F. T., Keon, N., Karreth, F., Eferl, R., Scheuch, H., Szremska, A., Amling, M., Schorpp-Kistner, M., Angel, P., and Wagner, E. F. (2004) Mice lacking JunB are osteopenic due to cell-autonomous osteoblast and osteoclast defects. *J. Cell Biol.* **164**, 613–623
45. Semerad, C. L., Christopher, M. J., Liu, F., Short, B., Simmons, P. J., Winkler, I., Levesque, J. P., Chappel, J., Ross, F. P., and Link, D. C. (2005) G-CSF potently inhibits osteoblast activity and CXCL12 mRNA expression in the bone marrow. *Blood* **106**, 3020–3027
46. Tatsumi, S., Ishii, K., Amizuka, N., Li, M., Kobayashi, T., Kohno, K., Ito, M., Takeshita, S., and Ikeda, K. (2007) Targeted ablation of osteocytes induces osteoporosis with defective mechanotransduction. *Cell Metab.* **5**, 464–475
47. Yang, D., Guo, J., Divieti, P., Shioda, T., and Bringhurst, F. R. (2008) CBP/p300-interacting protein CITED1 modulates parathyroid hormone regulation of osteoblastic differentiation. *Endocrinology* **149**, 1728–1735
48. Song, L., Liu, M., Ono, N., Bringhurst, F. R., Kronenberg, H. M., and Guo, J. (2012) Loss of wnt/ β -catenin signaling causes cell fate shift of preosteoblasts from osteoblasts to adipocytes. *J. Bone Miner. Res.* **27**, 2344–2358
49. Zanolini, S., and Canalis, E. (2014) Notch1 and Notch2 expression in osteoblast precursors regulates femoral microarchitecture. *Bone* **62**, 22–28
50. Hong, H. K., Chong, J. L., Song, W., Song, E. J., Jywook, A. A., Schook, A. C., Ko, C. H., and Takahashi, J. S. (2007) Inducible and reversible Clock gene expression in brain using the tTA system for the study of circadian behavior. *PLoS Genet.* **3**, e33
51. Chen, J., Shi, Y., Regan, J., Karuppaiah, K., Ornitz, D. M., and Long, F. (2014) Osx-Cre targets multiple cell types besides osteoblast lineage in postnatal mice. *PLoS One* **9**, e85161
52. Davey, R. A., Clarke, M. V., Sastra, S., Skinner, J. P., Chiang, C., Anderson, P. H., and Zajac, J. D. (2012) Decreased body weight in young Osterix-Cre transgenic mice results in delayed cortical bone expansion and accrual. *Transgenic Res.* **21**, 885–893
53. Ishizuya, T., Yokose, S., Hori, M., Noda, T., Suda, T., Yoshiki, S., and Yamaguchi, A. (1997) Parathyroid hormone exerts disparate effects on osteoblast differentiation depending on exposure time in rat osteoblastic cells. *J. Clin. Investig.* **99**, 2961–2970
54. Partridge, N. C., Kemp, B. E., Livesey, S. A., and Martin, T. J. (1982) Activity ratio measurements reflect intracellular activation of adenosine 3',5'-monophosphate-dependent protein kinase in osteoblasts. *Endocrinology* **111**, 178–183
55. Ferrari, S. L., Pierroz, D. D., Glatt, V., Goddard, D. S., Bianchi, E. N., Lin, F. T., Manen, D., and Boussein, M. L. (2005) Bone response to intermittent parathyroid hormone is altered in mice null for β -arrestin2. *Endocrinology* **146**, 1854–1862
56. Gesty-Palmer, D., Flannery, P., Yuan, L., Corsino, L., Spurney, R., Lefkowitz, R. J., and Luttrell, L. M. (2009) A β -arrestin-biased agonist of the parathyroid hormone receptor (PTH1R) promotes bone formation independent of G protein activation. *Sci. Transl. Med.* **1**, 1ra1